Building reconstruction from interferometric SAR data: potential and limits

U. Soergel, K. Schulz, U. Thoennessen
FGAN-FOM Research Institute for Optronics and Pattern Recognition, Germany

Keywords: SAR, Building, Detection, Reconstruction, Urban

ABSTRACT: The improved ground resolution of state of the art synthetic aperture radar (SAR) sensors suggests utilizing such data for the analysis of urban areas. An approach for the detection and reconstruction of buildings from InSAR data with about one meter spatial resolution is proposed and demonstrated. Reconstruction results for a rural and a built-up area are presented and discussed by comparison with ground truth like maps and high resolution DEM. Especially in inner city areas, remote sensing by SAR suffers from the consequences of the inherent side-looking illumination, such as occlusion of objects by more elevated objects interrupting the line of sight and signal layover of different objects with the same distance to the sensor. Furthermore, specular reflection and multi-bounce scattering lead to very strong signals, which superimpose the backscatter of large parts of their neighborhood. Geometric constraints of the impact of the mentioned SAR phenomena on the visibility of buildings are derived. Some of the mentioned limitations can be overcome with multi-aspect analysis, e.g. by filling occluded areas with data from other aspects and correcting layover effects. This is demonstrated for one scene covered from 3 InSAR data sets of different aspects.

1 INTRODUCTION

Three-dimensional city models are of great interest for visualization, simulation and monitoring purposes in different fields. Such 3D city models are usually derived from aerial imagery [Henricsson, 1996] or LIDAR data [Stilla and Jurkiewicz, 1999; Weidner and Foerstner, 1995]. The increasing resolution of SAR sensors opens the possibility to utilize such data for scene interpretation in urban areas as well. Approaches for a 3D building recognition from SAR and InSAR data have been proposed [Bolter, 2001; Gamba et al., 2000; Soergel et al., 2001]. Different SAR specific phenomena [Schreier, 1993] like foreshortening, layover, shadow, and multipath-propagation burden the scene interpretation or make it even impossible. These phenomena arise from the side-looking scene illumination of SAR sensors. Especially in dense built-up areas with high buildings, large portions of the data can be interfered by these illumination effects. The analysis of multi-aspect data offers the opportunity to alleviate these drawbacks, e.g. by filling occluded areas with data from other aspect directions.

For the building recognition task the typical appearance of buildings in the InSAR data is modeled. Their height and roof structure can be derived from the InSAR DEM or from the length and the size of the occluded shadow area cast from the building on the ground behind in the intensity image. Other hints to buildings are layover areas and bright linear double-bounce scatterers at the building footprint. Such context knowledge is exploited by a model-based iterative approach to detect and reconstruct buildings presented in this paper. Additionally, a geometric and topologic building model is required for the analysis, e.g. the preferred right-angled geometry of building structures. Besides simple buildings with rectangular footprint more complex footprint structures are considered as well.

In order to consider neighborhood relations an iterative approach is advantageous. Intermediate reconstruction results are used as reference for a simulation of InSAR data with respect to the parameters of

the given real data. Differences between the simulated and the real data control the iterative improvement of the reconstruction.
In Section 2 the SAR and InSAR techniques are introduced briefly. The appearance of buildings in the radar imagery is discussed in Section 3. Phenomena caused by side-looking illumination are explained and geometric relations for the determination of disturbed data are derived. The model-based approach for the detection and reconstruction of buildings is proposed and demonstrated for a rural and an urban scene in Section 4.

2 SENSOR PRINCIPLE

Side-looking SAR sensors are mounted on satellites or airplanes. The basic sensor principle is to illuminate large areas on the ground with the radar signal and to sample the backscatter. From the different time-of-flight of the incoming signal the range between the sensor and the scene objects is obtained. The analysis of single SAR images is usually restricted to the signal amplitude.
For interferometric SAR processing (InSAR) two SAR images are required, which were taken from different positions [Bamler and Hartl, 1998]. Due to the geometric displacement, the distances from the sensors to the scene differ, which results in a phase difference in the interferogram. Elevation differences in the scene are approximated by a linear function with these phase differences.
The accuracy of an InSAR DEM varies locally depending on the signal to noise ratio (SNR). The so-called coherence is a measure of the local SNR. Coherence is usually estimated from the data by a window-based computation of the magnitude of the complex cross-correlation coefficient of the SAR images. The noise sensitivity results often in `data holes´ or competing elevation values after the geocoding step with a forward transformation. Hence, the InSAR DEM data have usually to be further processed before geocoding.

3 APPEARANCE OF BUILDINGS IN SAR IMAGES

3.1 *Phenomena caused by side-looking illumination*

Fig. 1 illustrates typical effects in SAR images in the vicinity of buildings. The so-called layover phenomenon occurs at locations with steep elevation gradient facing towards the sensor, like vertical building walls (Figure 1a). If object areas located at different positions have the same distance to the sensor, like roofs (I), walls (II), and the ground in front of buildings (III), the backscatter is integrated to the same range cell. Layover areas appear bright in the SAR image (Figure 1 c).

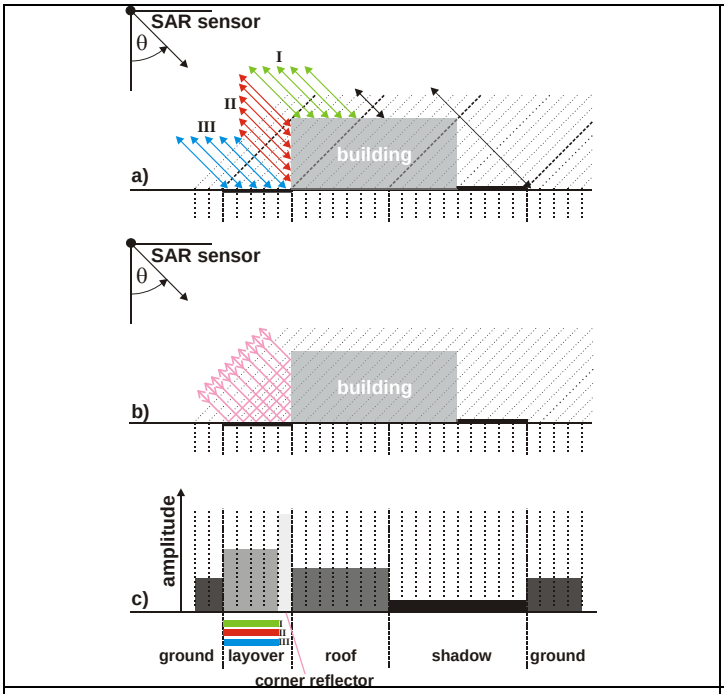

Fig. 1. SAR Phenomena at a flat roofed building. a) layover, b) corner reflector, c) SAR range line.

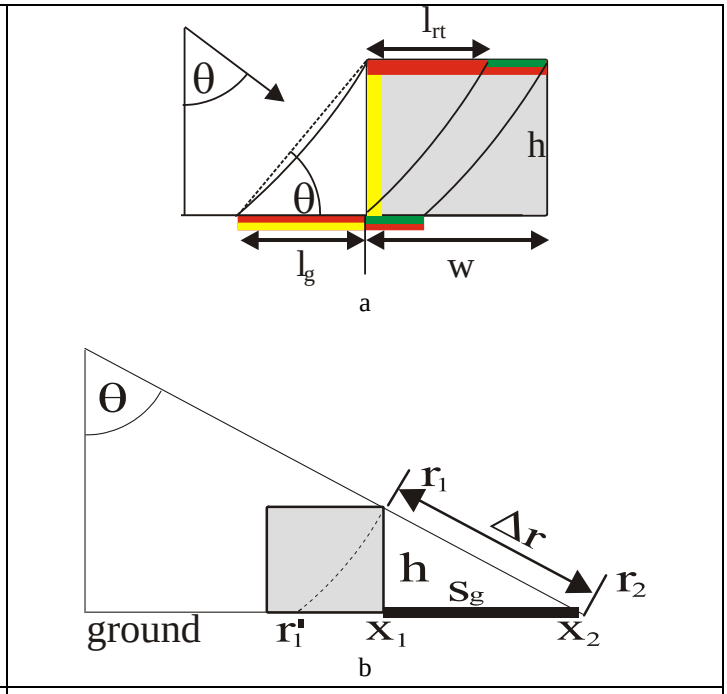

Fig. 2. a) Layover in front and on a flat roofed building, b) Shadow behind a building.

Perpendicular alignment of building faces towards the sensor leads to strong signal responses by double-bounce scattering at the dihedral corner reflector between the ground and the building wall (Fig. 1b). This results in a line of bright scattering in azimuth direction at the building footprint (Fig. 1c). At the opposite building side the ground is partly occluded from the building shadow. This region appears dark in the SAR image, because no signal returns into the related range bins.

3.2 *Geometric Constraints*

In this section the phenomena of layover and shadow are discussed in more detail. The sizes of the layover areas l_g and shadow areas s_g on the ground in range direction depend on the viewing angle θ and the building height h. The layover area (see Fig. 2a) is given by:

$$l_g = h \cdot \cot(\theta). \quad (1)$$

For the building analysis the roof area l_{rt} is of interest, which is influenced by layover. At the far side of a building with width w a part of the roof is not interfered with layover (shown in green in Fig. 2a), if the inequation is fulfilled:

$$h < w \cdot \tan(\theta). \quad (2)$$

In the case of shadow geometric relations can be obtained, too (Fig. 2b). The slant range shadow length Δr is the hypotenuse of the right-angled triangle with the two sides h and s_g. The building elevation h is given by:

$$h = \Delta r \cdot \cos(\theta). \quad (3)$$

A simple projection of the slant range SAR data on a flat ground plane (ground range), ignoring the building elevation, leads to a wrong mapping of the roofs edge r_1 to point r_1'. Starting from point r_2 the true position x_1 of the building wall can be determined (Bolter, 2001):

$$x_2 = r_2 \cdot \sin(\theta) \quad (4)$$

$$x_1 = x_2 - \Delta r \cdot \sin(\theta) \quad (5)$$

$$s_g = x_2 - x_1 = h \cdot \tan(\theta). \quad (6)$$

However, the shadow analysis can be reliable only, if the ground behind the building is flat and if no signal from other elevated objects propagates into the shadow area (e.g. a neighbored building).

Different building roof structures lead to special shapes of the cast shadow. Fig. 3 left illustrates the appearances of common building roof types in SAR amplitude or intensity images. The assumed illumination direction is from right to left. The shadow shape depends on the aspect. Flat roofed buildings cast usually stripe-like or L-shaped shadows. A building with pent roof structure (sloped roof) may cause a trapezoidal shadow. A gabled roof building may cast sexangle shaped shadow. But, both of the latter building types may lead to stripe-like or L-shaped shadow as well (e.g. if the range direction is top-down or bottom-up in Fig. 3).

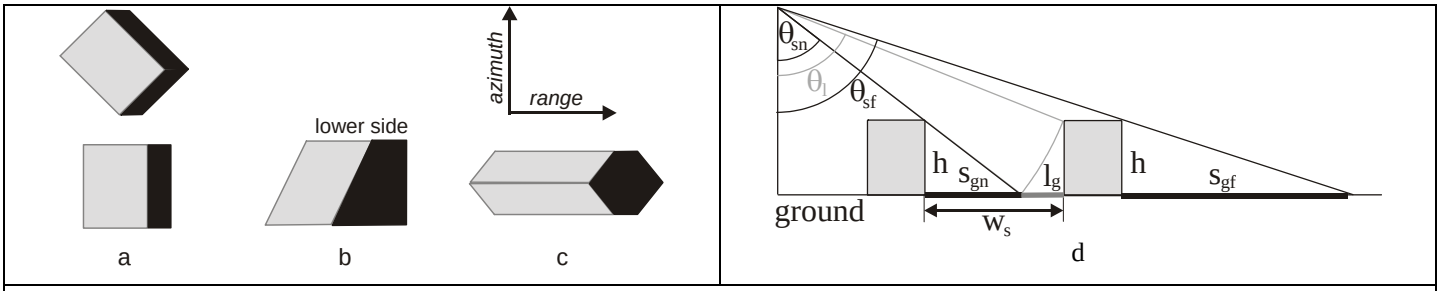

Fig. 3. Appearance of different buildings types in SAR amplitude or intensity images: a) flat roof, b) pent roof, c) gable roof, d) shadow and layover from buildings displaced in range direction.

The viewing angle increases in range direction over the swath. Assuming a range of the viewing angle θ between 40° and 60°, the shadow length of a certain building is more than doubled from near to far range. In Fig. 3d such a situation is depicted (shadow length s_{gn}, s_{gf}). A worst case will arise if a road between two building rows is orientated parallel to the sensor trajectory. The street is partly occluded from shadow and partly covered with layover. An object on the road can only be sensed properly, if a condition for the road width w_S holds:

$$w_s > s_{gn} + l_g = h \cdot (\tan(\theta_{sn}) + \cot(\theta_l)). \qquad (7)$$

4 TEST DATA

InSAR data of two different sites will be analyzed with respect to building detection and recognition. The first site is a rural area and the second one located in a built-up city.

4.1 *Rural Area*

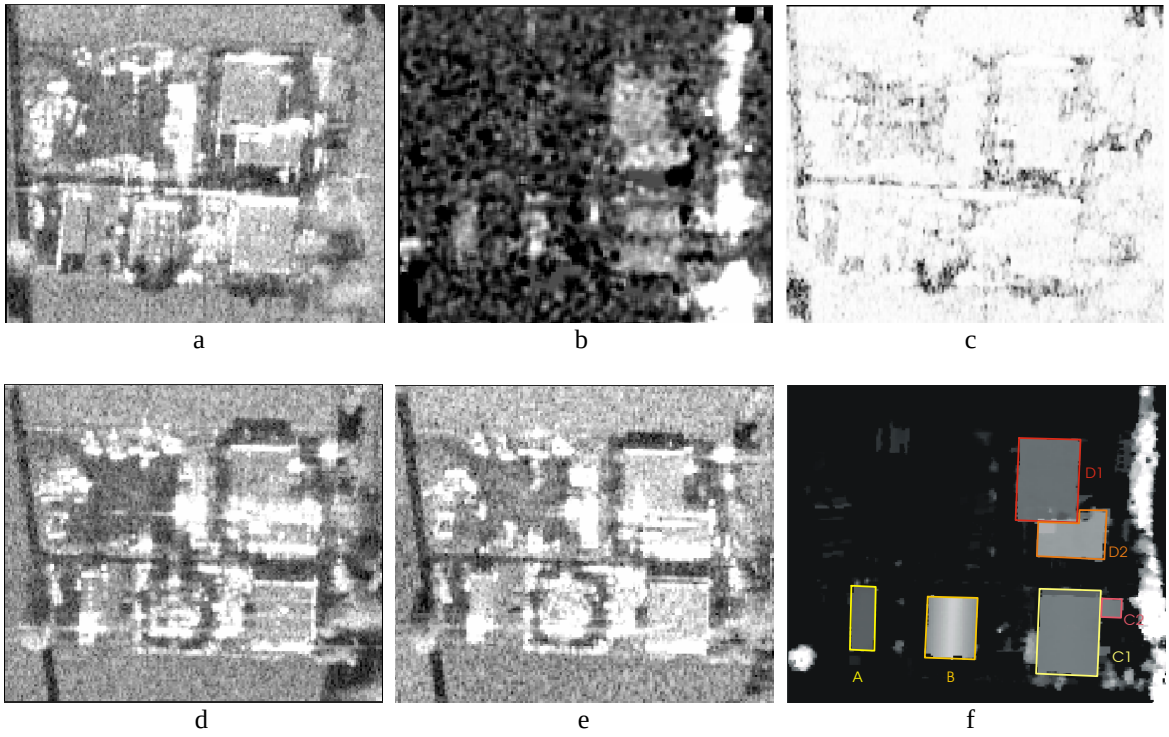

Fig. 4. Test data set Solothurn. a-c) InSAR illumination from north (a) intensity, b) DEM, c) coherence); d) ground truth: LIDAR data and building footprints; e,f) intensity of InSAR measurements from south with large (e) and small (f) off-nadir angle.

In Fig. 4 a small part of an InSAR data set of the test site measured from north is illustrated in the original slant range projection. The scene contains several buildings of different types in a rural area close to Solothurn, Switzerland. The ground truth data consisting of a LIDAR DEM and building footprints are shown in Fig. 4f. The InSAR data were recorded by the airborne DO-SAR system [Faller and Meier, 1993]. The center frequency of this X-band system is 9.5 GHz ($\lambda \approx 3$cm). The slant range data have a resolution of about 1.2m x 1.2m. Range direction is from top to down. Assuming a constant noise power, it is evident that in areas of the intensity image with low backscatter power (dark regions in Figure 4a) the SNR is poor. This results in low coherence (dark regions in Figure 4c) and distorted height data (Figure 4b). A standard deviation of the height data of about 1 m was estimated from a large flat grass area outside the presented area of the scene. Two additional InSAR data sets of the same scene were available, which have been acquired from south with two different off-nadir angles (Figure 4d,e).

4.2 *Built-up Area*

The Fig. 5a and 5b illustrate the intensity and height channel of an InSAR data set taken over an urban area (Karlsruhe, Germany). Range direction is bottom-up. The data have been recorded by the airborne AER-II experimental multi-channel SAR system [Ender, 1998]. This system is equipped with a phased array antenna and several receiver channels. The center frequency of this X-band system is 10 GHz with a maximum signal bandwidth of 160 MHz. In the slant range geometry shown here, the data have a resolution of approximately 1m in range and 0.5 m in azimuth direction. During the SAR measurements an aerial image in oblique view was taken (Figure 5c).

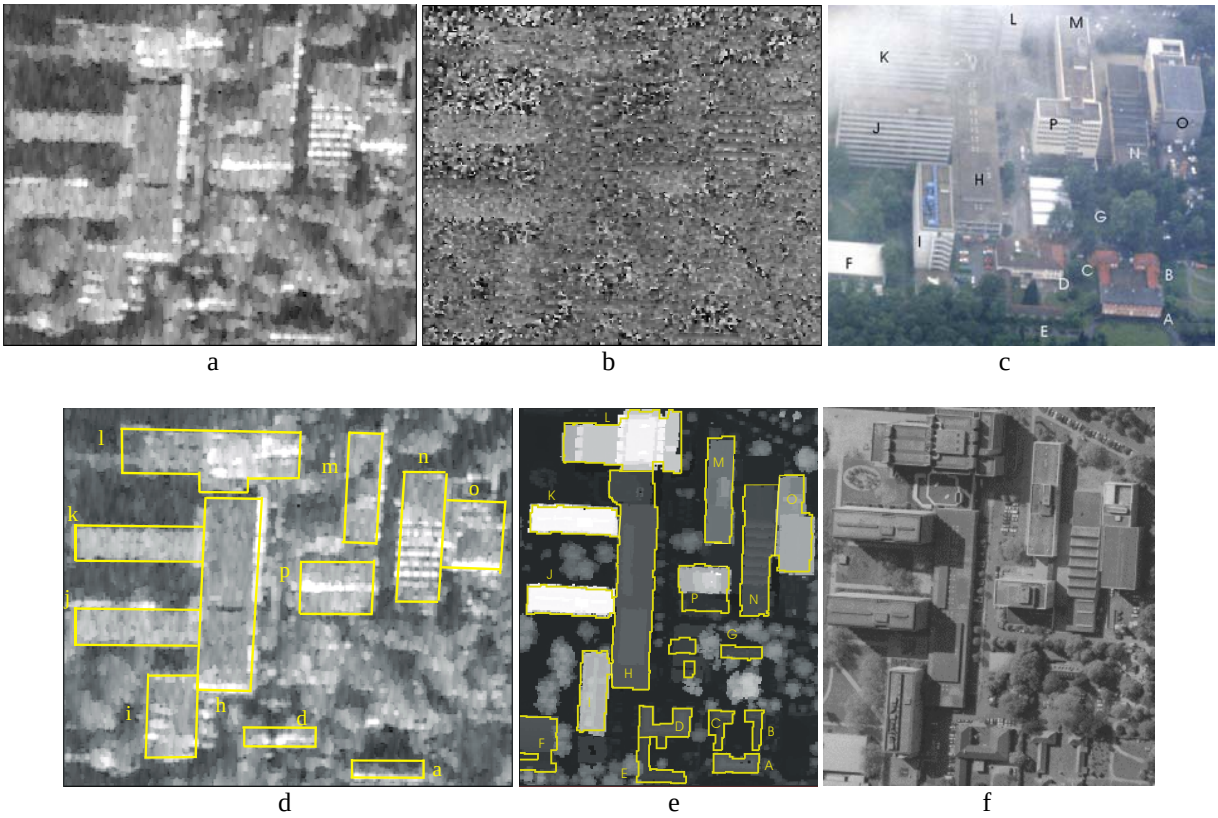

Fig. 5. InSAR slant range data and truth data: a) intensity, b) height, c) aerial image shot during InSAR measurement, d) “sensed truth”, e) LIDAR data and "ground truth”, f) aerial image in nadir view.

Fig. 5d shows again the intensity image overlaid with the building footprints drawn by a human operator without any context information of the scene. This information shall be called “sensed truth”. The comparison with the LIDAR DEM superimposed with ground truth footprints from a map (Fig. 5e) and the aerial image in nadir view (Fig. 5f) reveals that even a human operator cannot spot every building in the scene.
Especially small buildings are hardly visible or buildings which are covered by layover (e.g. from high trees). Scene interpretation from remote sensing imagery is a demanding task. The human ability to interpret even complex scenarios is usually not accomplished by automatic machine vision systems. Hence, the sensed truth represents a best effort result of any automatic approach.

5 APPROACH FOR BUILDING DETECTION AND RECONSTRUCTION FROM INSAR DATA

The detailed process for the detection and reconstruction of the buildings was described in [Soergel et al., 2003a] for the built-up area and in [Soergel et al., 2003a] for the rural scene. Here, a summery of the workflow is given.

The building recognition is performed iteratively by a production system [Niemann, 1990]. At least one InSAR data set is required. Detection and reconstruction of buildings are carried out in separated modules. The first step is the pre-processing of the InSAR data, e.g. smoothing and speckle reduction [Desnos and Matteini, 1993]. In the subsequent segmentation step primitive objects are extracted from the original slant

range InSAR data. This is advantageous in order to avoid artifacts due to the geocoding, e.g. the distorted appearance of building edges in the ground range projection. From primitive objects more complex objects (building hypotheses) are assembled in the detection module.

After projection of coordinates of these building candidates from slant range into the world coordinate system, a building recognition step follows. In this module model knowledge is exploited, e.g. the rectangular shape of buildings or their preferred parallel alignment along roads. If multi-aspect data are available, the sets of building candidates derived from the different data sets are fused.

Intermediate results are used for a simulation of the InSAR DEM, layover, shadow, and dihedral corner reflectors. The simulation results are re-projected to the SAR geometry and compared with the real data. Differences between the simulation and the real data control the update of the process: new building hypotheses are generated and false ones eliminated. Hence, the resulting scene description is expected to converge to the real 3D objects in the scene with increasing number of cycles. The processing stops either after a given maximum number of iterations or if the RMS of the difference between the simulated and the real InSAR DEM is smaller than a given threshold.

6 RESULTS

The result of the multi-aspect analysis of the Solothurn data is illustrated in red in Figure 6a. The ground truth (that is almost the same than the sensed truth) building footprints are depicted in white. No false positives have been detected. The main building boundaries were extracted. Building B was identified correctly as gabled roof building. The roof structure was derived mainly from the shadow analysis in this case. A 3D visualization of this result is shown in Figure 6b together with surrounding trees from the normalized InSAR DEM. The RMS of the corners of the building footprints is smaller than 3 m in x and y direction. The RMS of the mean elevation is about 1.5 m.

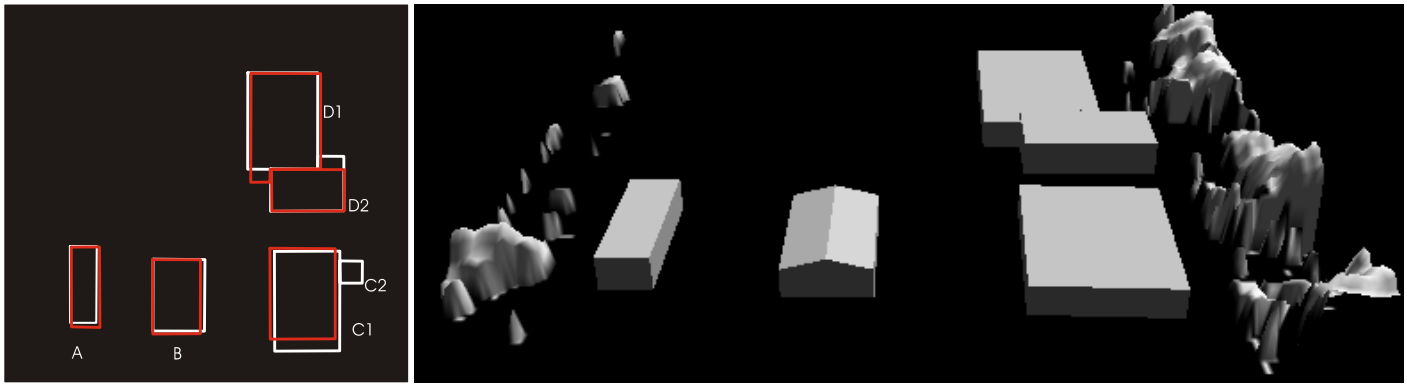

a b

Fig. 6. Final result for scene Solothurn: result (red) and truth (white), 3D visualization of a) with trees from InSAR DEM;

With respect to the assessment of the building detection for the urban scene Karlsruhe it is worthwhile to distinguish between sensed truth and ground truth. The performance of the proposed approach can be assessed based on the sensed truth (Fig. 5d). The comparison with the ground truth (Fig. 5e) gives insight in the feasibility of building detection and reconstruction in urban scenes with this approach using InSAR data of the given quality.

The result of the first iteration re-projected into the slant range after the reconstruction step is illustrated in Figure 7a (red rectangles). The shadow analysis did not yield good results, due to the proximity of the buildings and many trees in the scene. Therefore, the calculation of the building height based mainly on the InSAR height data. 13 buildings were detected.

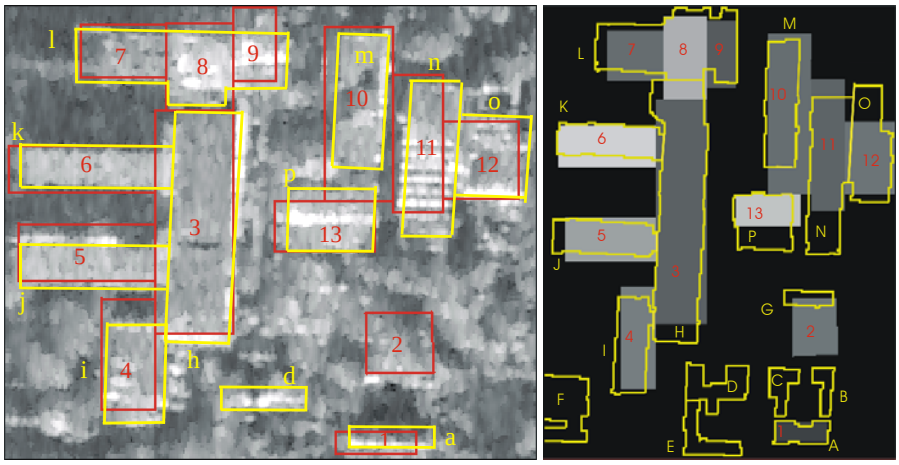

a b

Fig. 7. a) Result of first iteration re-projected into the slant range after the reconstruction step (red) and sensed truth, b) final result after 5 iterations (grey value coding of building height) superimposed with real ground truth.

The comparison with the sensed truth (yellow in Figure 7a) gives: 9 buildings are correct, one is missing (d) and one is over-segmented (l). The over-segmentation was caused from superstructures on the rooftop with significant different height. One false building is present (object 2) at the location of large trees. However, the mayor part of those buildings were detected which were labeled manually.
In Fig. 7b is the final result after five iterations illustrated. The grey level corresponds with the reconstructed building height. The real ground truth is superimposed in yellow. With respect to this ground truth, additional five buildings at the bottom of the scene are missing. The reason is in most of the cases occlusion or layover caused from high trees. Building G for example is not visible at all even in the aerial image shown in Figure 5c. However, mainly small buildings were not detected. Especially the height of tall buildings was underestimated. The buildings J and K on the left hand side are about 40 m high. But, their estimated height was 7 m smaller. Wrong height estimates lead to erroneous positions of the footprints after the forward transformation into the world coordinate system. The buildings appear shifted towards the sensor. The main parts of the two building complexes were detected. The recognition of the gabled roof of the small building A failed. It was reconstructed as flat roof building. Probably, this roof would not be reconstructed correct from this InSAR data set even in case the building was detached. The reason is the orientation of the building in azimuth direction which is disadvantageous for the shadow analysis. For a illumination from the right, better results could be expected.

7 CONCLUSION

The side-looking sensor principle of SAR is disadvantageous for the building reconstruction task. Especially in dense urban environments with tall buildings this task is often unfeasible. But, in case of suburban or rural scenes acceptable building reconstruction results can be achieved. Building features are detectable in the InSAR DEM and in the InSAR intensity. The coherence should be considered in order to avoid blunders. Occlusion and layover effects can be compensated by a multi-aspect analysis. This leads to a further improvement of the reconstruction quality. An iterative approach offers the opportunity of a stepwise consideration of the mutual interdependencies of the man-made objects. Furthermore, the evidence of building candidates is enhanced by a confirmation from analysis results of several data sets.

8 ACKNOWLEDGEMENT

We want to thank Dr. Schmid (Swiss Defence Procurement Agency) for providing the DO-SAR and LIDAR data of the Solothurn scene and Dr. Brenner and Prof. Ender from FGAN-FHR for the AER-II data of Karlsruhe.

REFERENCES

Bamler R, Hartl P (1998) Synthetic Aperture Radar Interferometry. Inverse problems, Vol. 14, No. 4, pp. 1-54.

Bolter R, (2001) Buildings from SAR Detection and Reconstruction of Buildings from Multiple View High Resolution Interferometric SAR Data. PhD thesis, University Graz, Austria.

Desnos Y L, Matteini. V (1993) Review on structure detection and speckle filtering on ERS-1 images. EARSeL Advances in Remote Sensing, Vol. 2, No. 2, pp. 52-65.

Faller N P, Meier E H (1995) First results with the airborne single-pass DO-SAR interferometer. IEEE Transactions on Geoscience and Remote Sensing, Vol. 33, No. 5, pp. 1230-1237.

Gamba P, Houshmand B, Saccini M (2000) Detection and Extraction of Buildings from Interferometric SAR Data. IEEE Transactions on Geoscience and Remote Sensing, Vol. 38, No. 1, pp. 611-618.

Henricsson O (1996) Analysis of Image Structures using Color Attributes and Similarity Relations, PhD Thesis, ETH Zuerich.

Niemann H (1990) Pattern Analysis and Understanding, Springer-Verlag, Berlin.

Schreier G (1993) Geometrical Properties of SAR Images. In: Schreier G (ed.) SAR Geocoding: Data and Systems. Wichmann, Karlsruhe, pp. 103-134.

Soergel U, Schulz K, Thoennessen U (2001) Phenomenology-based segmentation of InSAR data for building detection. In: Radig B, Florczyk S (eds.) Pattern Recognition, 23rd DAGM Symposium, Berlin: Springer, pp. 345-352.

Soergel U, Schulz K, Thoennessen U, Stilla U (2002) Utilization of 2D and 3D information for SAR image analysis in dense urban areas. Proc. 4th European conference on synthetic aperture radar, EUSAR 2002. Berlin: VDE, pp. 429-434.

Soergel U, Thoennessen U, Stilla U (2003a) Reconstruction of Buildings from Interferometric SAR Data of built-up Areas. In: Ebner H, Heipke C, Mayer H, Pakzad K (eds) Photogrammetric Image Analysis PIA'03, International Archives of Photo-grammetry and Remote Sensing, Vol. 34, Part 3/W8, pp. 59-64.

Soergel U, Thoennessen U, Stilla U (2003b) Iterative Building Reconstruction in Multi-Aspect InSAR Data. In: Maas HG, Vosselman G, Streilein A (eds) 3-D Reconstruction from Airborne Laserscanner and InSAR Data, International Archives of Photogrammetry and Remote Sensing, Vol. 34, Part 3/W13, pp. 186-192.

Stilla, U, Jurkiewicz, K (1999) Reconstruction of building models from maps and laser altimeter data. In: Agouris, P., Stefanidis, A. (eds.), Integrated spatial databases: Digital images and GIS, Berlin, Springer, pp. 34-46.

Weidner U, Foerstner W (1995) Towards Automatic Building Extraction from High Resolution Digital Elevation Models. ISPRS Journal, Vol. 50, No. 4, pp. 38-49.